Nuclear Physics A493 (1989) 112–123
North-Holland, Amsterdam

LOW-ENERGY CROSS SECTIONS FOR THE ^{6}Li(p, ^{3}He)^{4}He REACTION

J.U. KWON, J.C. KIM and B.N. SUNG

Physics Department, Seoul National University, Seoul 151-742, Korea

Received 30 September 1988

Abstract: Differential and total cross sections for the ^{6}Li(p, ^{3}He)^{4}He reaction at proton energies between 120 keV and 505 keV have been measured. The ^{6}Li+p elastic scattering also has been measured and used as a cross section standard. The total cross section shows a weak structure at $E_p \sim 400$ keV. The astrophysical S-function defined as $\sigma_{tot} = [S(E)/E] \exp(-2\pi\eta - gE)$ is well represented by a constant value 2.97 ± 0.03 MeV · b.

E NUCLEAR REACTIONS ^{6}Li(p, ^{3}He), $E = 120$–505 keV; measured $\sigma(E_p, \theta)$; deduced $\sigma(E)$, astrophysical S-factor.

1. Introduction

The ^{6}Li(p, ^{3}He)^{4}He reaction at sub MeV region is of considerable astrophysical interest. It has a large cross section for the destruction of the ^{6}Li and affects the universal abundance of lithium which is a prime factor in the theories concerning the origin of the light element in astrophysics [1]).

Recently, this reaction has been also of much concern in the controlled thermonuclear reactor (CTR) program. The ^{6}Li becomes the new candidate of the advanced fusion fuel in CTR [2]). But detailed evaluation for the performance of an advanced fuel system such as ^{6}Li(fuel)+p(catalyzer) requires an accurate knowledge of the absolute reaction cross section at energies from $E_p \sim 100$ keV to a few MeV [3-5]).

The total cross sections for the ^{6}Li(p, ^{3}He)^{4}He reaction have been measured by many authors [3-15]) in the energy range from $E_p = 25$ keV to several MeV. Previous results are summarized in fig. 1. This figure shows that there is a convergence at energies below 300 keV. However, a large spread of experimental results still exists at energies above 300 keV. For example, near the region $E_p = 1.8$ MeV resonance, the data of Marion *et al.* [12]) are about 1.4 times the data of Lin *et al.* [13]). Of particular interest are the discrepancies between two recent results obtained in the region $300 \leqslant E_p \leqslant 700$ keV; the data of Shinozuka *et al.* [11]) are about 10% higher than those of Elwyn *et al.* [4]).

The present work was undertaken to clarify these discrepancies, and the experiments were performed at proton energies 120 keV $\leqslant E_p \leqslant$ 505 keV. In the present experiment the spectra of elastically scattered protons and helium particles from

0375-9474/89/$03.50

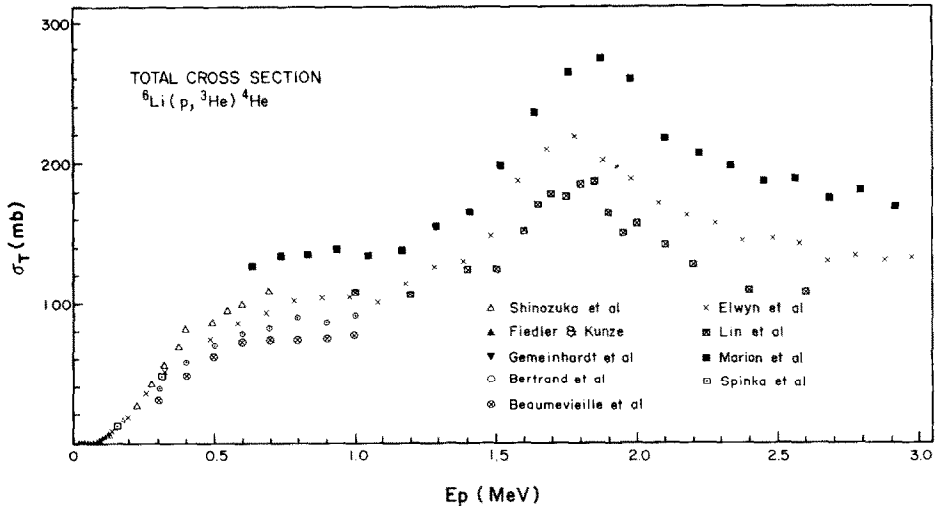

Fig. 1. Previously measured total cross sections for the $^{6}Li(p, {}^{3}He)^{4}He$ reaction at energies below 3 MeV as given in refs. [3,4,6,7,9-13]).

the $^{6}Li(p, {}^{3}He)^{4}He$ reaction have been taken simultaneously and the reaction cross sections are derived from the measured yields by using the relation

$$\left(\frac{d\sigma}{d\Omega}\right)_{\text{reaction}} = \frac{{}^{3}\text{He yield}}{\text{proton yield}} \left(\frac{d\sigma}{d\Omega}\right)_{\text{elastic}} . \tag{1}$$

The reaction cross sections obtained in this way are free from the errors associated with the target thickness and composition, beam charge measurements, and the detector solid angle.

The cross sections for the $^{6}Li+p$ elastic scattering necessary for this procedure have also been measured in the present work.

2. Experiment

The present experiment was performed with the H^{+} beam from the Seoul National University 0.4 MV Van de Graaff accelerator*. Fig. 2 shows the floor plan of the beam transport. After magnetic analysis and collimation by a 2 mm diameter molybdenum diaphragm, the beam was allowed through the target and come to rest under vacuum on the Faraday cup. The Faraday cup was made of a 30 cm long × 3 cm diameter pyrex glass tube lined with 0.13 mm thick copper foil. An in-line LN_2 cold trap was installed in front of the target chamber with an extended cold finger in order to reduce carbon deposits on the target. The 15° analysing magnet was calibrated by a measurement of the resonance reactions $^{11}B(p, \alpha)$ [E_r = 163 keV], $^{19}F(p, \alpha\gamma)$ [E_r = 340.6 keV], and $^{31}P(p, \gamma)$ [E_r = 440 keV] [16]). The E-slit at

* Product of High Voltage Engineering Corp., model LC-400.

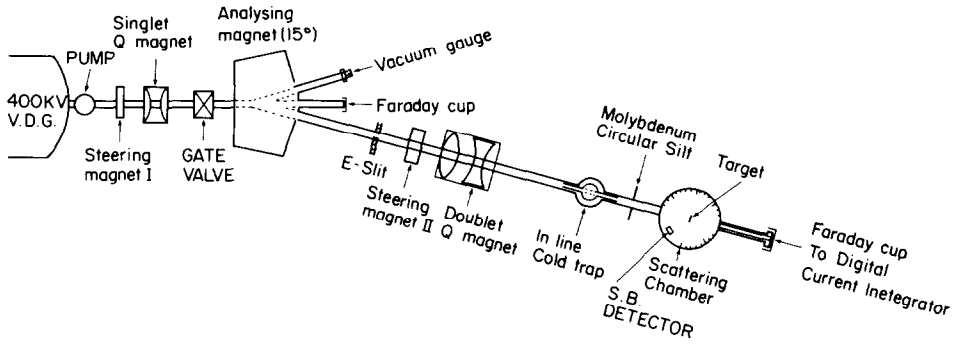

Fig. 2. Floor plan of the Seoul National University Van de Graaff accelerator and beam transport system.

the exit of the analysing magnet was 3 mm wide, which gave rise to an energy spread (FWHM) of approximately 10 keV. However, the reproducibility of the centroid energy was within ±3 keV.

The targets were prepared by evaporating LiF enriched* to 99.3% in ^{6}Li onto a 10 $\mu g/cm^2$ carbon backing. The thickness of the targets was ranging from 3 $\mu g/cm^2$ to 12 $\mu g/cm^2$, for which the corresponding beam energy losses at $E_p = 300$ keV are 1.5 keV and 6 keV respectively. Two 300 μm silicon surface barrier detectors were used; one mounted on a movable arm and one fixed at the $\theta_{lab} = 90°$. The solid angle subtended by the detectors, defined by collimators placed at the entrance face, was approximately 3 msr.

Spectra were accumulated on ND66 multi-channel analyser. The beam currents used were about 10 nA and the dead time losses were kept below 1%. An ORTEC digital integrator was used for the beam charge measurement. This has been calibrated with a standard cell and resistor to an accuracy better than 0.3%.

3. Results

3.1. ^{6}Li+p ELASTIC SCATTERING

In the present experiment the proton yields from the ^{6}Li+p elastic scattering and the reaction products from the $^6Li(p, ^3He)^4He$ reaction were measured simultaneously. A typical spectrum taken at $E_p = 400$ keV is shown in fig. 3. The differential cross sections for the $^6Li(p, ^3He)^4He$ reaction were then obtained by making use of the cross sections for the ^{6}Li+p elastic scattering. The ^{6}Li+p elastic scattering has been studied previously by McCray [17]) at the region $E_p > 400$ keV. This result shows that the elastic cross sections have no resonances below $E_p \sim 1.0$ MeV and that at lower energies they are roughly approaching to the Rutherford values. In order to obtain the elastic cross sections for the region $E_p < 400$ MeV and to improve the

* Oak Ridge National Laboratory Products.

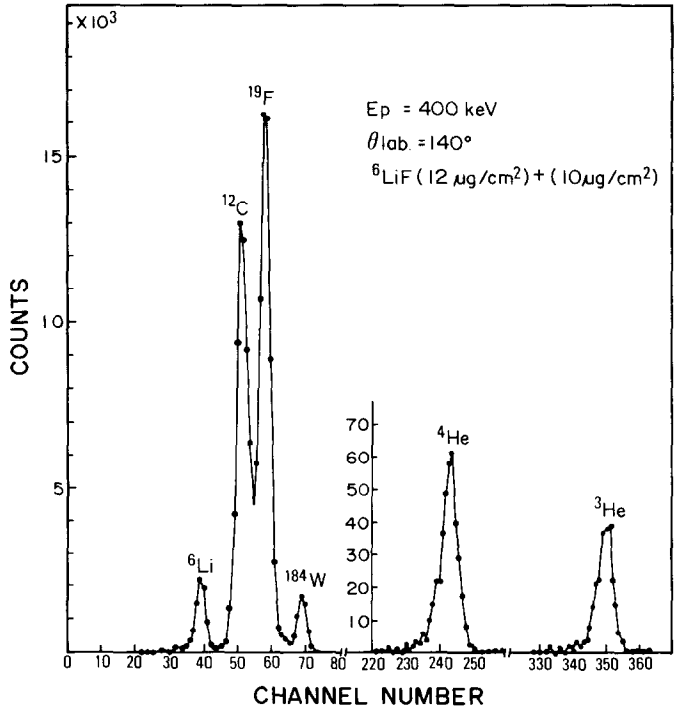

Fig. 3. A typical pulse-height spectrum of the charged particles from reactions of protons with ^{6}LiF on C backings. The peaks labeled ^{3}He and ^{4}He are from the ^{6}Li(p, ^{3}He)^{4}He reaction, while the others represent elastically scattered protons.

accuracy of McCray's data at low energies, we have plotted, from our measured ^{6}Li + p elastic data, $[(Y/Q)/\sigma(\theta)_{\mathrm{Ruth}}]$ versus E_{p} as shown in fig. 4. The quantity in the bracket denotes the yields of elastically scattered protons per beam charge normalized to the Rutherford cross section. The curve is flat below $E_{\mathrm{p}} \sim 350$ keV. However, it rises slowly at higher energies and at $E_{\mathrm{p}} = 500$ keV the elastic cross section is 8.5% larger than the Rutherford cross section.

3.2. DIFFERENTIAL CROSS SECTIONS AT $\theta_{\mathrm{lab}} = 140°$

Differential cross sections for the ^{6}Li(p, ^{3}He)^{4}He reaction in the range of $E_{\mathrm{p}} = 120$ to 505 keV have been measured at $\theta_{\mathrm{lab}} = 140°$ and are shown in fig. 5. The measurements were repeated four times using targets of various thicknesses of 3 to 12 μg/cm^{2}. The error bar of each points in fig. 5 incorporates the statistical error for the ^{3}He yields, the error caused by the peak analysis to obtain elastic proton yields from the spectra, and an error of 5% estimated to arise from the beam energy spread. It should be mentioned that the ^{6}Li elastic peak and the ^{12}C elastic peak were not separated well at the energies $E_{\mathrm{p}} < 240$ keV. Therefore, the differential cross sections

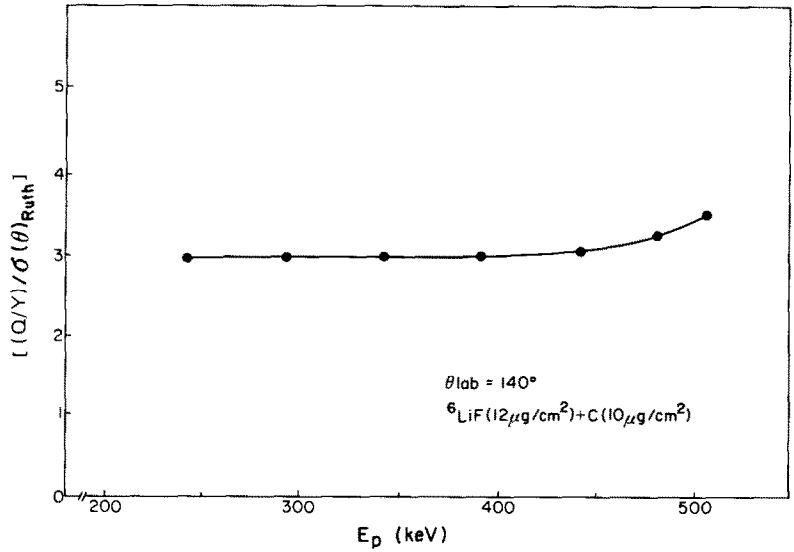

Fig. 4. The yields of elastically scattered protons per beam charge normalized to the Rutherford cross section versus E_p. Deviations from the Rutherford cross section can be seen at $E_p \gtrsim 350$ keV. The ordinate scale is arbitrary.

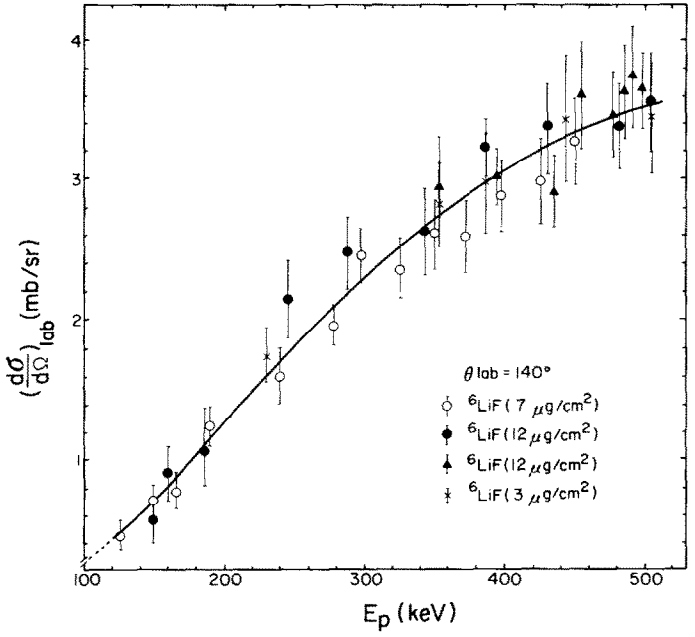

Fig. 5. Differential cross sections for the $^{6}Li(p, ^{3}He)^{4}He$ reaction at $\theta_{lab} = 140°$ measured with targets of various thicknesses. The solid line represents the result of the least-square fit to the eq. (2) in the text.

in this region were obtained by the relative yield measurements only. At these low proton energies the beam divergence after going through the target was severe due to the multiple scattering, and deteriorated the charge collection efficiency of the Faraday cup. This effect has been corrected by a similar measurement of the charge collection efficiency as a function of proton energies previously carried out by Shinozuka *et al.* [11]). Fig. 6 shows the results of the charge-collection efficiency measurement in the present experiments.

Background ^{4}He particles were observed at $E_p \sim 340$ keV from the $^{19}F(p, \alpha\gamma)$ resonance reaction. However, 2.1 MeV ^{3}He particles from the $^{6}Li(p, {}^{3}He)^{4}He$ reaction and 1.8 MeV ^{4}He particles from the $^{19}F(p, \alpha\gamma)$ reaction have been well separated in the spectrum by using 2 to 6 keV thick LiF targets.

The solid line in fig. 5 is the result of the least-square fit of the present data to the curve shape

$$\frac{A}{E}\exp\left(-\frac{B}{\sqrt{E}}-CE\right), \tag{2}$$

which is also used to extract the astrophysical S-factors. This curve with $A = 93.3 \pm 6.7$, $B = 2.59 \pm 0.03$, $C = 0.637 \pm 0.071$ has then been incorporated to obtain the total cross sections.

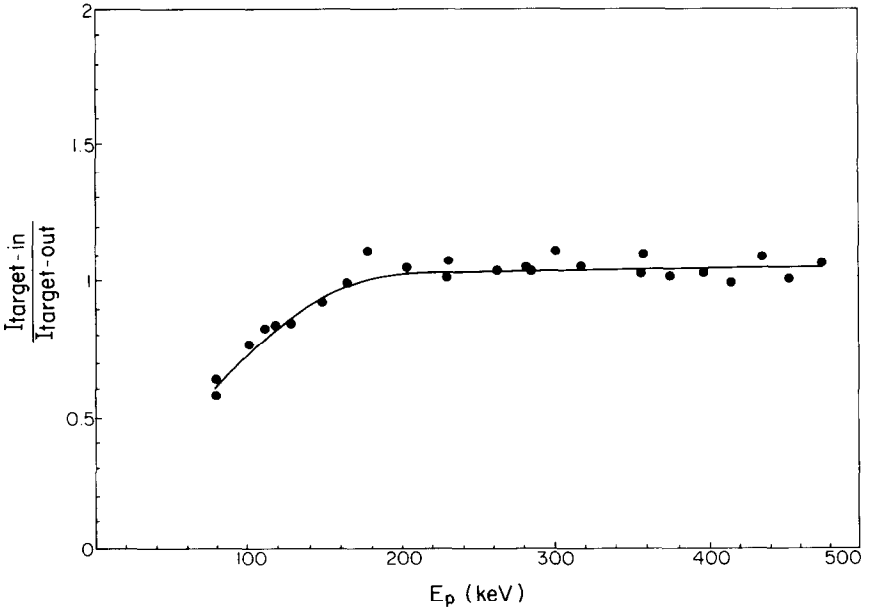

Fig. 6. The beam charge-collection efficiencies of the Faraday cup. $I_{\text{target-out}}$ is the beam current measured at the Faraday cup in the absence of the target. $I_{\text{target-in}}$ is the beam current measured in the presence of the target.

3.3. ANGULAR DISTRIBUTIONS OF THE ^{6}Li(p, ^{3}He)^{4}He REACTION

The angular distributions of the ^{6}Li(p, ^{3}He) reaction were measured for ten energies at $E_p = 125$ keV to 505 keV. For each energy, measurements were made at 6 angles between $\theta_{lab} = 40°$ and 140°. The yields of ^{4}He particles were also incorporated for the angular distribution data of the ^{6}Li(p, ^{3}He)^{4}He reaction by use of the appropriate kinematic relationship [18]). The differential cross section at each angle was obtained by normalizing to those at $\theta_{lab} = 140°$. The results are plotted in fig. 7 and the error shown represents only the statistical error arising from the angular distribution measurements. The angular distributions were least square fitted with a Legendre polynomial expansion up to order 2,

$$\frac{d\sigma}{d\Omega} \cong B_0 + B_1 P_1(\cos\theta_{c.m.}) + B_2 P_2(\cos\theta_{c.m.}) . \tag{3}$$

The results of the least square fits are listed in table 1 and plotted in fig. 7 with solid lines. The errors for the total cross sections $\sigma_T = 4\pi B_0$ in table 1 are the quadratic sums of the angular distribution errors and the errors quoted for the differential cross sections at $\theta_{lab} = 140°$ in the sect. 3.2.

4. Discussion

4.1. TOTAL CROSS SECTION

The total cross sections for the ^{6}Li(p, ^{3}He)^{4}He reaction as obtained in the present experiment are shown in fig. 8. The present results are in an excellent agreement with most recent measurements of Elwyn *et al.* [4]) and Shinozuka *et al.* [11]) in the region of $E_p \leq 300$ keV. In the region of 400 keV $\leq E_p \leq$ 500 keV there has been an apparent discrepancy of approximately 10% between the above two measurements. However, the present results agree well with both of them; the results at 390 keV agree with those at 375 keV and 400 keV of ref. [11]) and the results at 442 keV and 505 keV are consistent with the result of ref. [4]) at 490 keV and the result of ref. [11]) at 500 keV. The present results for the total cross sections of the ^{6}Li(p, ^{3}He)^{4}He reaction show the presence of a weak resonance at $E_p \sim 400$ keV. This resonance behavior should be attributed to the large negative value of B_2 coefficient as appeared in fig. 9. The same large negative B_2 value at $E_p \sim 400$ keV has been seen in the work of ref. [11]) and also in the earlier experiment by Beaumevielle *et al.* [15]). Beaumevielle *et al.* [19]) have suggested as the $J^\pi = \frac{3}{2}^-$ state of ^{7}Be with the corresponding excitation energy $E_x = 5.90$ MeV. However, it should be noted that this resonance was not observed in the ^{6}Li + p elastic scattering [17]), ^{3}He + ^{4}He scattering [20,21]) and proton capture [22,23]). The mirror counterpart, though a level at $E_x = 5.3$ MeV in ^{7}Li was suggested by Mani and Dix [24]) from their ^{7}Li(p, p')^{7}Li experiment, has also been in dispute for many years [25]).

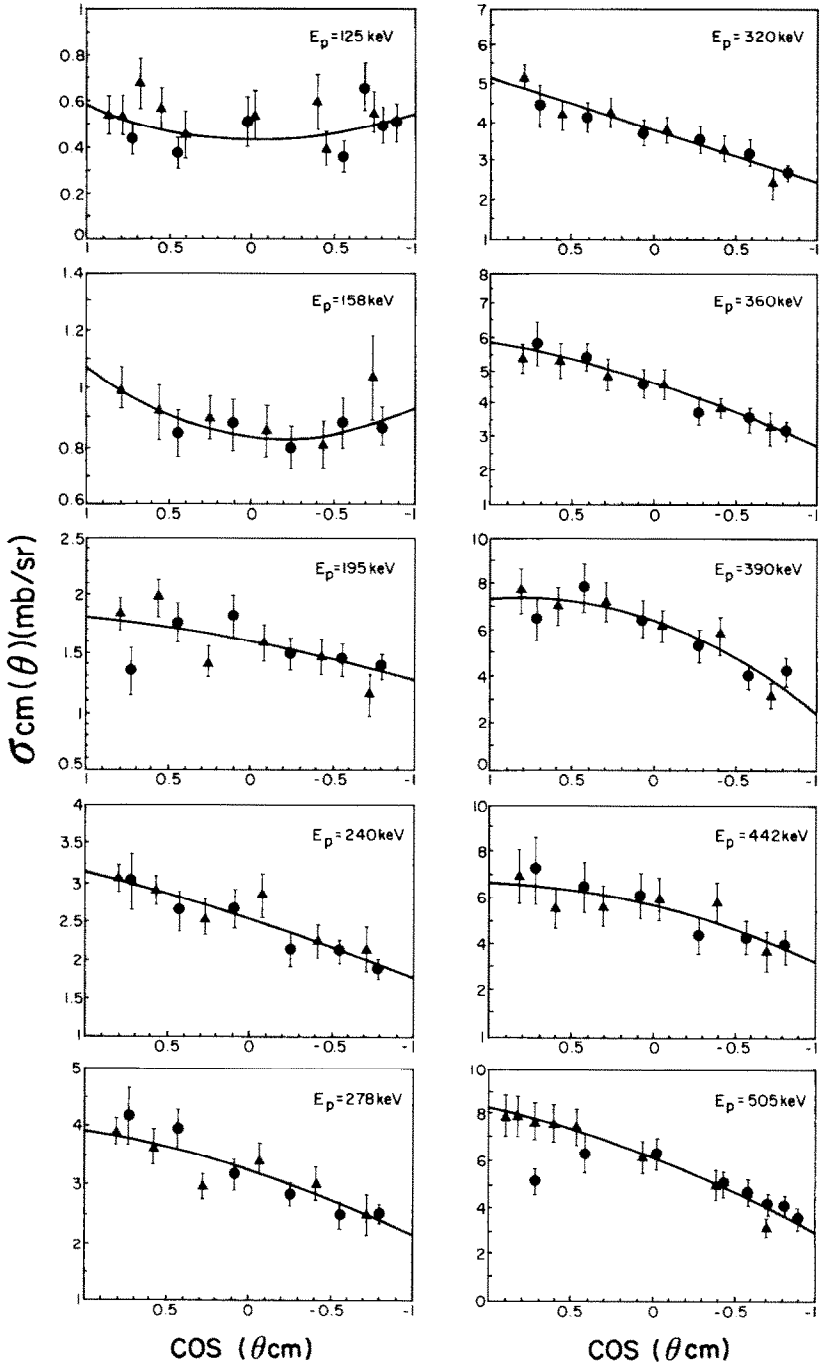

Fig. 7. Angular distributions of the ^{3}He particles for the $^{6}Li(p, ^{3}He)^{4}He$ reaction at the proton energies indicated. The solid lines represent the result of the Legendre polynomial fit. The points denoted by ▲ were obtained from the ^{4}He yield by use of appropriate kinematic relationships, while the solid circles were obtained from the ^{3}He yields.

TABLE 1

Coefficients of Legendre polynomial fitting and integrated total cross section, and astrophysical S-factor

E_p (keV)	B_1/B_0 (mb/sr)	B_2/B_0 (mb/sr)	σ_T (mb)	$S(E)$ (MeV · b)
125	0.011	0.183	580 ± 1.43	2.97
158	0.069	0.124	11.05 ± 2.09	2.86
195	0.166	−0.021	19.74 ± 2.70	3.02
240	0.274	−0.014	31.14 ± 3.71	3.07
278	0.296	−0.0002	39.10 ± 2.91	2.94
320	0.338	−0.002	48.91 ± 4.09	2.93
360	0.335	−0.0035	56.52 ± 4.16	2.86
390	0.411	−0.172	74.20 ± 5.59	3.39
442	0.316	−0.077	68.28 ± 5.73	2.70
505	0.443	−0.054	80.68 ± 6.06	2.80

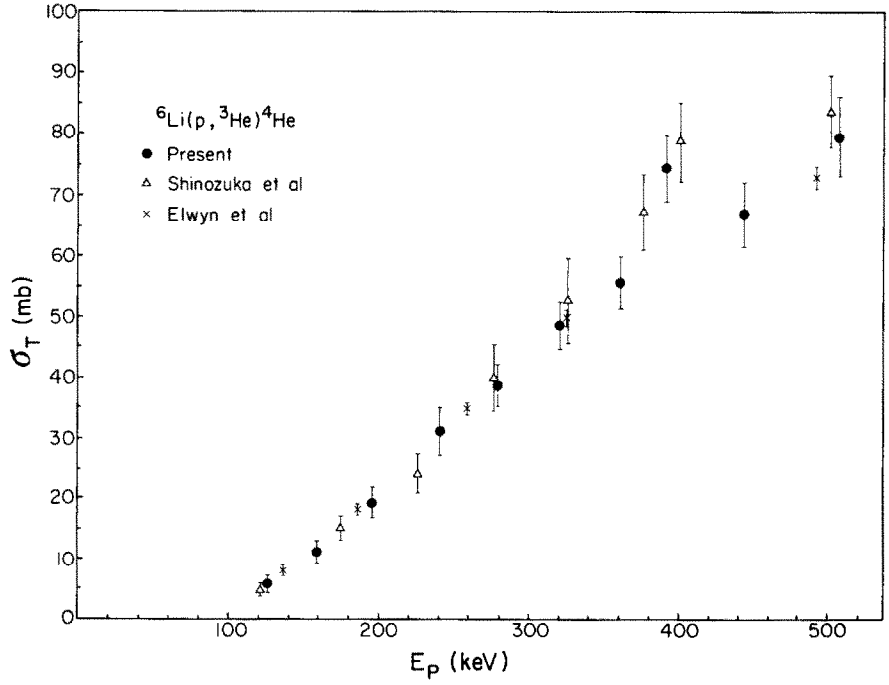

Fig. 8. The total cross sections for the $^{6}Li(p, ^{3}He)^{4}He$ reaction. The present results denoted by solid circles are compared with results of two recent measurements of refs. [4]) and [11]).

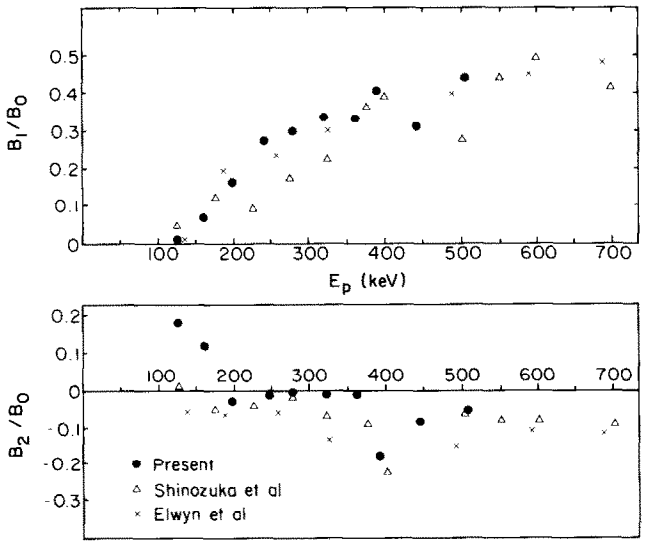

Fig. 9. The ratios of Legendre polynomial coefficients B_L/B_0 for the $^{6}Li(p, ^{3}He)^{4}He$ reaction, compared with the two recent results of refs. [4]) and [11]).

4.2. THE ASTROPHYSICAL *S*-FUNCTION

To evaluate the astrophysical *S*-function, which is a convenient parameter to extrapolate the total cross sections to energies of astrophysical interest, we have used the expression used by Spinka *et al.* [3]) and Shinozuka *et al.* [11]), i.e.,

$$\sigma_{tot} = \frac{S(E)}{E} \exp(-2\pi\eta - gE), \tag{4}$$

where

$$2\pi\eta = \frac{2\pi Z_1 Z_2 e^2}{\hbar v} = \frac{2.758}{\sqrt{E}}, \tag{5}$$

$$g = 0.122\left(\frac{AR^3}{Z_1 Z_2}\right)^{1/2}, \qquad A = \frac{A_1 A_2}{A_1 + A_2}, \tag{6}$$

$$R = r_0(A_1^{1/3} + A_2^{1/3}). \tag{7}$$

Taking $r_0 = 1.3$ fm, the same value used by previous authors, we have obtained the *S*-function as shown in fig. 10. Also shown in the same figure are results of Shinozuka *et al.* [11]) and Elwyn *et al.* [4]) together with results quoted in ref. [11]). The data of Elwyn *et al.* [4]) were derived from their tabulated data of total cross section.

The present results in fig. 10, with an exception of the weak structure-associated point at $E_p = 390$ keV, show that the *S*-function is well represented, within the errors, by a constant value. All other data show qualitatively the same behavior except those of Elwyn *et al.* [4]), which clearly show the presence of a non-negligible slope.

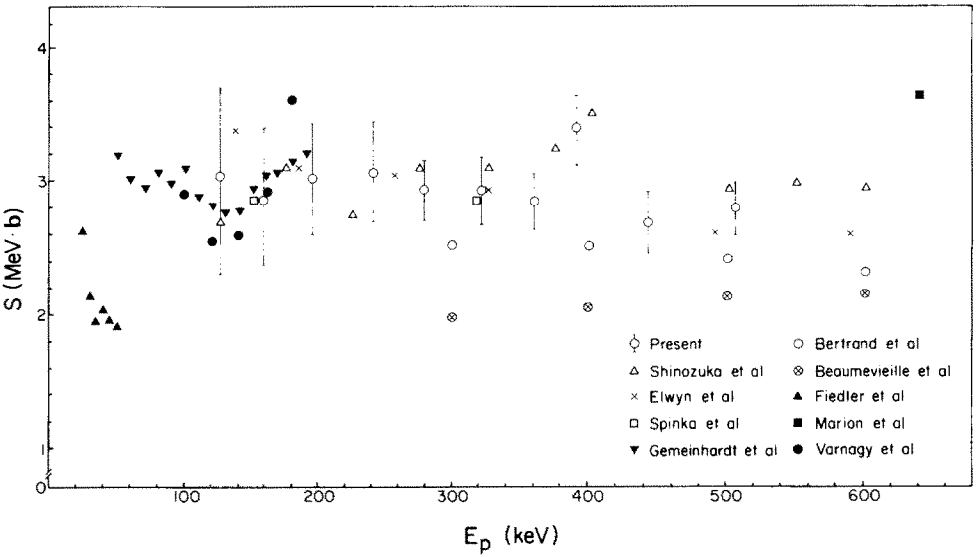

Fig. 10. The experimental astrophysical S-functions derived from eq. (4) in the text using $r_0 = 1.3$ fm.

This is by far the most significant difference between the result of Elwyn *et al.* [4]) and the result of Shinozuka *et al.* [11]), and the present result agrees better with the latter in this respect.

The least-squares fit result for the constant S-factor obtained from the present experiment alone is 2.93 ± 0.08 MeV · b. This value is in good agreements with previous results 3.0 MeV · b, 3.2 MeV · b, and 2.85 MeV · b of ref. [11]), ref. [6]), and ref. [3]) respectively. However, the least-squares fit by using the data of refs. [3,4,6,11]) and the present one altogether gave rise to the result 2.97 ± 0.03 MeV · b.

References

1) A. Audouze and H. Reeves, Astrophys. J. **158** (1969) 419
H. Reeves, Nuclear reactions in stellar surfaces and their relations with stellar evolution (Gordon and Breach, London, 1971)
2) J.R. McNally, Jr., Nucl. Fusion **11** (1971) 187
3) H. Spinka, T. Tombrello and H. Winkler, Nucl. Phys. **A164** (1971) 1
4) A.J. Elwyn, R.E. Holland, C.N. Davids, L. Meyer-Schutzmeister, F.P. Mooring and W. Ray, Jr., Phys. Rev. **C20** (1979) 1984
5) C.R. Gould, R.O. Nelson, J.R. Williams and J.R. Boyce, Nucl. Sci. Eng. **55** (1974) 267
6) W. Gemeinhardt, D. Kammke and C. von Röneck, Z. Phys. **197** (1974) 267
7) O. Fiedler and P. Kunze, Nucl. Phys. **A96** (1967) 513
8) M. Várnagy, J. Csikai, J. Szabó, S. Szegedi and J. Bänhalmi, Nucl. Instr. Meth. **119** (1974) 451
9) F. Bertrand, G. Grenier and J. Pornet, unpublished CEA-R-3428 (1968)
10) H. Beaumevieille, unpublished CEA-R-2624 (1964)
11) T. Shinozuka, Ph.D thesis, Tohoku Univ. (unpublished);
T. Shinozuka, Y. Tanaka and Y. Sugiyama, Nucl. Phys. **A326** (1979) 47
12) J.B. Marion, G. Weber, and F.S. Mozer, Phys. Rev. **104** (1956) 1402

13) C.S. Lin, W.S. Hou, M. Wen and J.C. Chen, Nucl. Phys. **A275** (1977) 93
14) G.P. Johnston and D.G. Sargood, Nucl. Phys. **A224** (1974) 349
15) H. Beaumevieille and N. Longequeue, Compt. Rend. **256** (1963) 1494
16) F. Ajzenberg-Selove, Nucl. Phys. **A433** (1985) 1; **A392** (1983) 1;
P.M. Endt and C. Van der Leun. Nucl. Phys. **A310** (1978) 1
17) J.A. McCray, Phys. Rev. **130** (1963) 2034
18) J.B. Marion and F.C. Young, Nuclear reaction analysis: graphs and tables (North-Holland, Amsterdam, 1968) p. 140
19) H. Beaumevieille, J.P. Longequeue, N. Longequeue and R. Bouchez, J. de Phys. **25** (1964) 933
20) T.A. Tombrello and P.D. Parker, Phys. Rev. **130** (1963) 1112
21) R.J. Spiger and T.A. Tombrello, Phys. Rev. **163** (1967) 964
22) J.B. Warren, T.K. Alexander and G.B. Chadwick, Phys. Rev. **101** (1956) 242
23) S. Bashkin and R.R. Carlson, Phys. Rev. **97** (1955) 1245
24) G.S. Mani and A.D.B. Dix, Nucl. Phys. **A106** (1967) 251
25) L. Brown and C. Petitjean, Nucl. Phys. **A117** (1968) 343